SASP

Homework 4

Homework 4 Report

Students

Riccardo Iaccarino
10868500
Xinmeng Luan
10876787

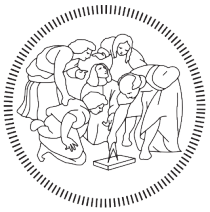

POLITECNICO
MILANO 1863

Introduction

Starting from the reference analog circuit, the WDF model comes as a discretization in which linear elements become input-output blocks and topological interconnections are replaced with MIMO junctions. Both those components will be characterized by a pair of wave variables a_n and b_n, which, together with the reference port resistance Z_n, will allow us to link their electrical quantities v_n and i_n. We can rely on two pairs of equations, for direct and inverse mapping respectively:

$$a_n = v_n + Z_n i_n \qquad b_n = v_n - Z_n i_n \tag{1}$$

$$v_n = \frac{a_n + b_n}{2} \qquad i_n = \frac{a_n - b_n}{2Z_n} \tag{2}$$

In the scheme depicted in Fig. 1 it is possible to see how we chose to implement the WDF model of the crossover network. In particular we opted for the use of just 3-port junctions, so that computation complexity is reduced. Moreover we divided the circuit into 3 different subcircuits corresponding to the sections that constitute the three filters (low-pass, band-pass, high-pass). Regarding the choice of the root, it is pretty straightforward since the only non-adaptable element of the network is the ideal voltage source.

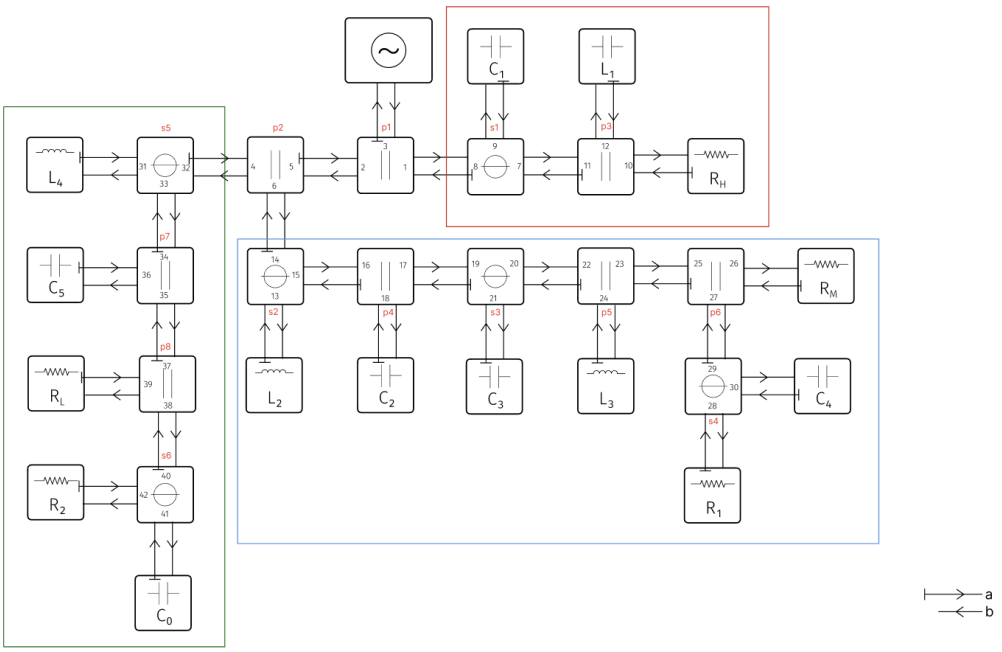

Figure 1: WDF scheme: the circuit is divided into high, mid and low sections.

All the linear elements have been adapted (as can be seen by the T-shaped stubs) following the *trapezoidal rule*, which returns a set of adaptation condition, depending on the considered component:

$$Z_i = R \qquad Z_i = \frac{T_s}{2C_i} \qquad Z_i = \frac{2L_i}{T_s} \tag{3}$$

where R_i is the resistance C_i the capacitance and L_i the inductance of the element. Scattering relations also depend on the component and link reflected and incident waves together (we set

it this way so that we refer to the ports of our junctions and not to the linear components):

$$a_i[k] = 0 \qquad a_i[k] = b_i[k-1] \qquad a_i[k] = -b_i[k-1] \tag{4}$$

In our case, the scattering relations are as follows:
High section:

$$a_9[k] = b_9[k-1] \qquad a_{12}[k] = -b_{12}[k-1] \qquad a_{10}[k] = 0 \tag{5}$$

Mid section:

$$a_{13}[k] = -b_{13}[k-1] \qquad a_{18}[k] = b_{18}[k-1] \qquad a_{21}[k] = b_{21}[k-1] \tag{6}$$
$$a_{24}[k] = -b_{24}[k-1] \qquad a_{26}[k] = 0 \qquad a_{28}[k] = 0 \tag{7}$$
$$a_{30}[k] = b_{30}[k-1] \tag{8}$$

High section:

$$a_{31}[k] = -b_{31}[k-1] \qquad a_{36}[k] = b_{36}[k-1] \qquad a_{39}[k] = 0 \tag{9}$$
$$a_{42}[k] = 0 \qquad a_{41}[k] = b_{41}[k-1] \tag{10}$$

For the junctions instead we made each port reflection-free using the two well-know equations for series and parallel connections coming from Kirchhoff's theory:

$$Z_s = Z_a + Z_b \qquad Z_p = \frac{Z_a Z_b}{Z_a + Z_b} \tag{11}$$

To do so we implemented two separate Matlab functions that allowed us to keep a readable and organized code. The adaption conditions for our case are listed in table 1.
Finally, scattering matrices must be computed to relate the reflected and the incident wave in a 3-port junction. The general relation (for a junction with ports 1-2-3) is:

$$\begin{bmatrix} b_1[k] \\ b_2[k] \\ b_3[k] \end{bmatrix} = \mathbf{S} \begin{bmatrix} a_1[k] \\ a_2[k] \\ a_3[k] \end{bmatrix} \tag{12}$$

The scattering matrix S depends on whether the junction represents a series or a parallel connection. For a 3-port series adaptor we have:

$$\mathbf{S}_s = \begin{bmatrix} 1 & 0 & 0 \\ 0 & 1 & 0 \\ 0 & 0 & 1 \end{bmatrix} - \frac{2}{Z_1 + Z_2 + Z_3} \begin{bmatrix} Z_1 \\ Z_2 \\ Z_3 \end{bmatrix} \begin{bmatrix} 1 & 1 & 1 \end{bmatrix} \tag{13}$$

whereas for the dual case, the parallel adaptor, we can compute it with admittances ($G = 1/Z$):

$$\mathbf{S}_p = \frac{2}{G_1 + G_2 + G_3} \begin{bmatrix} G_1 \\ G_2 \\ G_3 \end{bmatrix} \begin{bmatrix} 1 & 1 & 1 \end{bmatrix} - \begin{bmatrix} 1 & 0 & 0 \\ 0 & 1 & 0 \\ 0 & 0 & 1 \end{bmatrix} \tag{14}$$

Once we collected all these variables, we can proceed with the operations of *forward* and *backward scan*, that are fundamental in computing the time course of our waves.
The final output is then plotted to valid the implementation of the WDF, as shown in Fig. 2.

	1-port elements	Adaptors
High section	$Z_{10} = R_H$ $Z_{12} = \frac{2L_1}{T_S}$ $Z_9 = \frac{T_S}{2C_1}$	$Z_7 = Z_{11} = \frac{Z_{10}Z_{12}}{Z_{10}+Z_{12}}$ $Z_8 = Z_7 + Z_9$
Mid section	$Z_{30} = \frac{T_S}{2C_4}$ $Z_{28} = R_1$ $Z_{26} = R_M$ $Z_{24} = \frac{2L_3}{T_S}$ $Z_{21} = \frac{T_S}{2C_3}$ $Z_{18} = \frac{T_S}{2C_2}$ $Z_{13} = \frac{2L_2}{T_S}$	$Z_{27} = Z_{29} = Z_{28} + Z_{30}$ $Z_{23} = Z_{25} = \frac{Z_{26}Z_{27}}{Z_{26}+Z_{27}}$ $Z_{20} = Z_{22} = \frac{Z_{23}Z_{24}}{Z_{23}+Z_{24}}$ $Z_{19} = Z_{20} + Z_{21}$ $Z_{17} = Z_{13}$ $Z_{15} = Z_{16} = \frac{Z_{17}Z_{18}}{Z_{17}+Z_{18}}$ $Z_{14} = Z_{15} + Z_{13}$
Low section	$Z_{41} = \frac{T_S}{2C_6}$ $Z_{42} = R_2$ $Z_{39} = R_L$ $Z_{36} = \frac{T_S}{2C_5}$	$Z_{38} = Z_{40} = Z_{41} + Z_{42}$ $Z_{35} = Z_{37} = \frac{Z_{38}Z_{39}}{Z_{38}+Z_{39}}$ $Z_{33} = Z_{34} = \frac{Z_{35}Z_{36}}{Z_{35}+Z_{36}}$ $Z_{32} = Z_{31} + Z_{33}$
General circuit		
$Z_4 = Z_{32}$ $\quad Z_6 = Z_{14}$ $Z_5 = \frac{Z_4 Z_6}{Z_4+Z_6}$ $\quad Z_1 = Z_8$ $Z_2 = Z_5$ $\quad Z_3 = \frac{Z_1 Z_2}{Z_1+Z_2}$		

Table 1: Adaptation conditions.

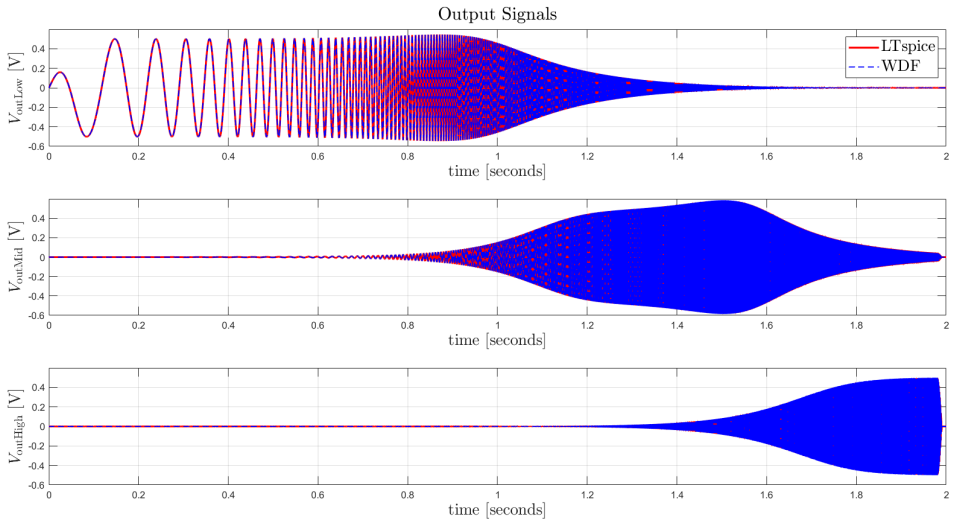

Figure 2: Output signals of the LTSpice simulation and the implemented WDF.

Question 1

From the obtained results shown in Fig. 3 the first noticeable difference between the three outputs is the amplitude. Indeed the error of the low-pass filter is the smaller of the three and it scales of a power of 10 until the least accurate filter, the high-pass. In terms of peaks, another interesting behaviour that characterizes the LPF is that the maximum error is achieved between 0.9 and 1 s, whereas the other two filters perform at their worst towards the end of the sweep. This is probably due to the bandwidth of the filters, in particular a common trend is a greater error towards the tail of the response.

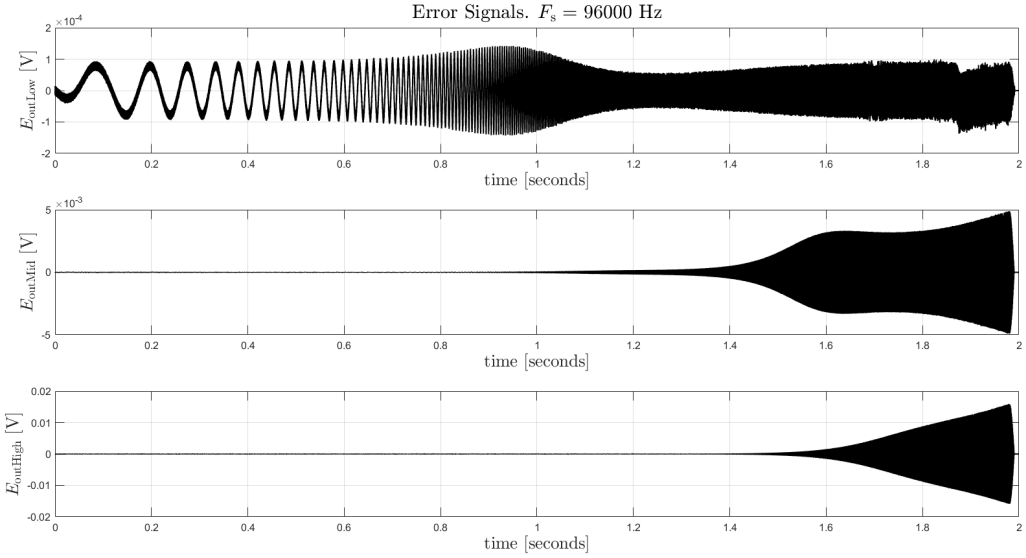

Figure 3: Error signals sensed at the three drivers.

The distinction in terms of accuracy is driven by the method of discretization used, in our case the *trapezoidal rule*, which maps frequencies from a continuous-time domain context to a discrete-time domain one. From this technique we can derive the following relation, also called *warping mapping*:

$$\omega = \frac{2}{T_s} tan\left(\tilde{\omega}\frac{T_s}{2}\right) \tag{15}$$

for which ω is closer to $\tilde{\omega}$ at low frequencies, differently from the high end of the spectrum. This behaviour is the main cause of the different magnitude of our filters' errors.

Question 2

As previously stated in eq.(15), the continuous-time related frequency depends on T_s, which is directly related to the sampling frequency ($F_s = 1/T_s$). This means that increasing F_s will improve the error, since the difference between the two variables decreases with it. To support our theoretical statements, we have plotted the errors for different values of sampling frequency in Fig. 4.

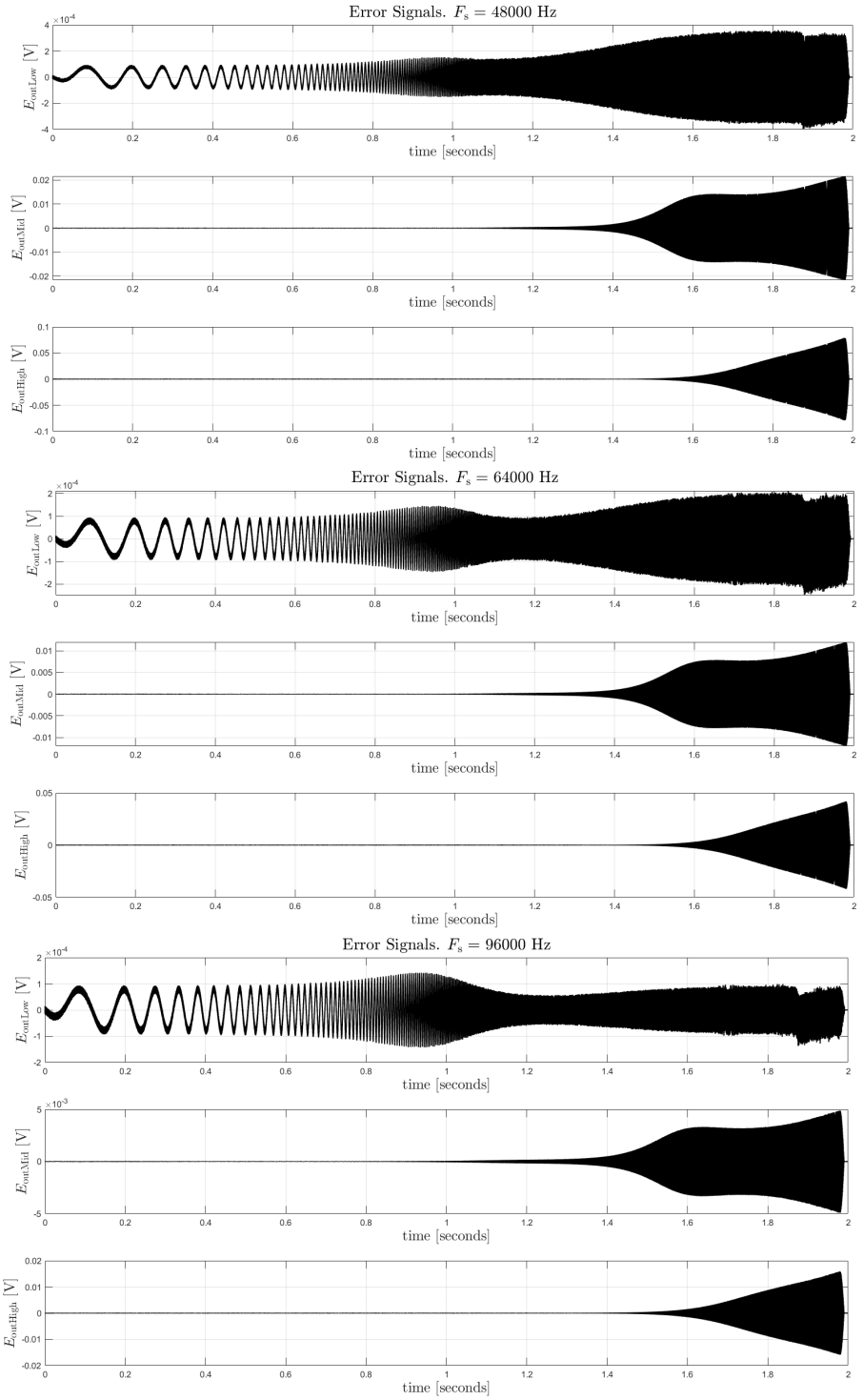

Figure 4: Errors of the output signals of the three drivers computed at different sampling frequencies (48kHz, 64kHz, 96kHz).

We can observe that for the middle and high frequencies elements the only difference is the amplitude of the error; a peculiar behaviour can be noticed instead comparing the three plots of the LPF: when the input signal is at low frequencies, the discretization is very accurate, indeed the error is very similar in all of the cases.

Question 3

Adding a single diode in parallel with the tweeter resistor R_H introduces a nonlinear component into the circuit. In this case, there would be two components that could not be adapted in the structure: the ideal voltage source and the diode. The scattering junction equations need to be updated to account for the new diode. The diode's nonlinear behavior should be incorporated into the equations, considering its v+, v- curve by graphical method. When solving the system of equations derived from the scattering junction functions, the iteration problem may be involved, which loses the main concept of WDFs, the explicit representation of the filter structure. Obviously, the presence of the diode will affect the filter's overall behavior. It may introduce nonlinear distortions, alter the frequency response, or affect other performance metrics.

Regarding the replacement of the ideal voltage source with a resistive voltage source, now the voltage source could be taken as a linear one-port element, as shown in Fig. 5. Therefore, we could take the diode as the root of the structure, instead of the voltage source. From that point on, the implementation of the WDF should just start again following the same passages depicted in the introduction. As a reference, the binary connection tree structure shown in the slide (Modeling and Implementation of Wave Digital Filters) (Fig. 6) should keep the same concept.

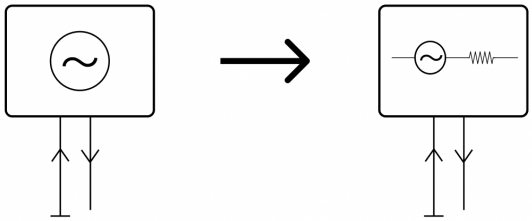

Figure 5: The representation of ideal voltage source and resistive voltage source.

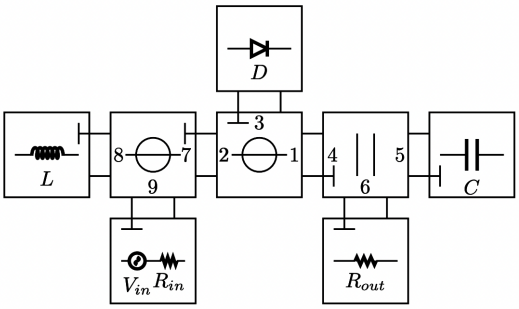

Figure 6: Binary Connection Tree.

Question 4

Starting from the continuous-time domain constitutive equation of an inductor, we can easily get the corresponding Laplace transform:

$$v(t) = L\frac{di}{dt} \longrightarrow V(s) = sLI(s) \tag{16}$$

We can now apply the *Backward Euler Method* that maps the s variable in the digital domain as $s \leftarrow \frac{1-z^{-1}}{T_s}$. The resulting equation is:

$$v[k] = \left(\frac{1-z^{-1}}{T_s}\right) Li[k] \tag{17}$$

Where we can see z^{-1} as a delay operator, which will lead us to the following:

$$v[k] = \frac{L}{T_s}i[k] - \frac{L}{T_s}i[k-1] \tag{18}$$

that is just a special case of the well-known constitutive equation of linear one-port elements:

$$v[k] = R_e[k]i[k] + V_e[k] \tag{19}$$

in which $R_e[k] = \frac{L}{T_s}$ is a resistance and $V_e[k] = -\frac{L}{T_s}i[k-1]$ is a voltage bias.
Substituting the equations (2) in the (19) and solving for $b[k]$, we can get to the scattering relation:

$$b[k] = \frac{R_e[k] - Z[k]}{R_e[k] + Z[k]}a[k] + \frac{2Z[k]}{R_e[k] + Z[k]}V_e[k] \tag{20}$$

The adaptation conditions that eliminate the instantaneous dependency of $b[k]$ from $a[k]$ are:

$$b[k] = V_e[k],\ Z[k] = R_e[k] \qquad \text{in our case} \rightarrow \qquad b[k] = -\frac{L}{T_s}i[k-1],\ Z[k] = \frac{L}{T_s} \tag{21}$$

Finally we can compute $i[k-1]$ following eq.(2) and substitute into the expression of $b[k]$:

$$b[k] = -\frac{L}{T_s}\left(\frac{a[k-1] - b[k-1]}{2Z[k]}\right) = -\frac{a[k-1] - b[k-1]}{2} \tag{22}$$

We can collect the information about the WD inductor model based on Backward Euler Method in the table below.

Constitutive Eq	**Wave Mapping in Case of Adaption**	**Adaptation Condition**
$v(t) = L\frac{di(t)}{dt}$	$b[k] = -\frac{a[k-1]-b[k-1]}{2}$	$Z[k] = \frac{L}{T_s}$

Table 2: Mapping and adaptation for inductors (Backward Euler Method)